Meccanica (2013) 48:545–553
DOI 10.1007/s11012-012-9614-6

Analytical and experimental investigation on friction of non-conformal point contacts under starved lubrication

Fadi Ali · Ivan Křupka · Martin Hartl

Received: 13 January 2012 / Accepted: 15 September 2012 / Published online: 5 October 2012

Abstract This paper presents an analytical and experimental study on the friction of non-conformal point contacts (ball-on-disk) under starved lubrication. Theoretical models were developed to simulate the behavior of friction and separation versus the degree of starvation while experimental measurements were conducted by using a Tribometer equipped with a torque sensor and a digital camera, which provided the possibility to use the optical interferometry technique simultaneously with measuring the friction. The effect of air-oil meniscus distance from the center of Hertzian contact on the friction between non-conformal surfaces was observed under starved conditions in sliding motion by capturing interferometric images. In addition, the reduction of friction by artificially-produced shallow micro-dents was investigated under severely starved and fully flooded conditions. Results show that the coefficient of friction increases dramatically when the air-oil meniscus starts to touch the circle of Hertzian contact and there is not such a significant difference in the friction between starved and fully flooded contacts since the air-oil meniscus is far away from the borders of Hertzian contact. In other words, the starvation of lubrication causes a high level of fatigue and wear of machine components when there is interference between the air-oil meniscus and the Hertzian contact. However, it was found that shallow micro-dents are helpful in reducing the friction under severe starvation conditions while the benefits of micro-dents are negligible for fully flooded conditions.

Keywords Friction · Non-conformal · Starved lubrication · Micro-dents

F. Ali (✉) · I. Křupka · M. Hartl
Department of Mechanical Engineering, Brno University of Technology, Brno, Czech Republic
e-mail: fa77f@yahoo.com

1 Introduction

A lot of machine components work with non-conformal point contacts such as gears, rolling-element bearings, cams, etc. The pressure in such concentrated contacts reaches high values according to the theory of Hertz in solid contacts, so that lubrication is needed to avoid wear and metal-to-metal contact. The separation between mating surfaces depends on the film thickness of lubrication and it is well known that the EHL regime is dominated in non-conformal point contacts where the theory of EHL can successfully predict the film thickness under fully flooded lubrication [1, 2]. In reality it is difficult to keep the rubbing surfaces under fully flooded lubrication, e.g., in cases of severe operating conditions (high speed, high load, high temperatures, start and reverse motion) or in cases where grease is used to lubricate rolling bearings. In previous cases the phenomenon of starved lubrication can be encountered and the film thickness may collapse to

just a few nanometers at high degrees of starvation, which in turn may result in component failure.

Wedeven *et al.* [3] used the technique of optical interferometry to investigate the phenomena of ball bearing starvation and the reduction of film thickness due to the failure of pressure build-up in the contact. The pressure in the inlet region of starved contact can be defined on the basis of a study that was performed by Elrod [4, 5], who developed a model using the parameter θ (fractional film content) representing the ratio between the oil thickness and the gap. Chiu [6] used a ball-flat rig test to study the starvation in roiling contact systems, obtained results showed that the starvation is attributed to the insufficiency of fluid replenishment on the track. Pemberton and Cameron [7] presented a study of fluid replenishment in EHL contacts and it was found that the balance between the entrained and the lost oil around the contact determines the position of inlet meniscus from the Hertzian contact. Chevalier *et al.* [8] performed a numerical study of starved EHL point contacts and the amount of oil on the surfaces was adopted to define the degree of starvation. Recent experimental studies about the effect of starvation on the film thickness of point contacts were carried out by Lubrecht *et al.* [9] and Cann *et al.* [10]. Numerical results by Damiens *et al.* [11] showed that the degree of starvation depends on operating conditions and the available amount of oil. The behavior of traction in starved EHL point contacts under rolling and sliding conditions was experimentally observed by Wedeven [12] and Querlioz *et al.* [13], the significance of these works is that the traction depends on the degree of starvation. Yang *et al.* [14] performed a numerical analysis on the traction of starved EHL line contacts and it was indicated that the traction increases rapidly at high degrees of starvation.

The proper modification of surface topography helps in reducing the friction between mating surfaces. For example, creating micro-dents on the surface, with proper dimensions and edges, reduces the interaction between asperities by emitting some amount of lubricant in the contact which results in enhancing the film thickness, contact fatigue life, wear resistance and reducing the friction. On the other hand, a reduction in film thickness with deep micro-dents was investigated under sliding motion due to the induction of cavitation and the increase of pressure fluctuation in the vicinity of micro-dent; see references [17–24]. Dumont *et al.* [25] described numerically the behavior of micro pits in the fully flooded and starved ball-on-disk contact and it was revealed that the benefits of micro pits decrease as the degree of starvation decreases because the film thickness becomes larger and the emitted amount of oil from micro-pits becomes negligible in comparison with the available amount of oil in the contact.

However, a lot of efforts focused on studying the effect of micro-dents on the film thickness formation and pressure distribution, while there is still a need to clarify the direct effect of micro-dents on the friction coefficient of non-conformal contacts under starved lubrication in sliding motion.

2 Theory

Many factors have an influence on the friction coefficient of EHL point contacts, such as rheological properties of lubricant, the slide-to-roll ratio, the thermal effect and so on. However, the Newtonian shear stress is given by;

$$\tau = \eta \Delta u / h \tag{1}$$

where τ is the shear stress [Pa], η is the dynamic viscosity of the lubricant [Pa s], Δu is the sliding velocity between the contacting surfaces [m/s] and h is the film thickness [m].

The traction force F is defined by the following;

$$F = \int_{r_c=0}^{r_c=a} \tau \, dA = \int_{r_c=0}^{r_c=a} \eta(\Delta u / h) 2\pi r_c dr_c \tag{2}$$

where F is the traction force [N], r_c is the radius of contact [m] and a is the radius of Hertzian contact [m].

The finite area dA of a circular point contact is given by;

$$dA = 2\pi r_c dr_c \tag{3}$$

The Barus equation in Ref. [15], predicts the viscosities as a function of pressure by the following form;

$$\eta = \eta_0 \exp(\alpha p_h) \tag{4}$$

where η_0 is the viscosity at atmospheric pressure [Pa s], α is the pressure-viscosity coefficient [1/Pa] and p_h is the Hertzian pressure [Pa s].

The Hertzian pressure is dominated in EHL point contacts and it is given by;

$$p_h = p_{\max}\left(1-(r_c/a)^2\right)^{1/2} = \left(3w/2\pi a^2\right)\left(1-(r_c/a)^2\right)^{1/2} \quad (5)$$

where $p_{\max}$ is the maximum pressure [Pa] and w is the normal load [N].

If we accept that the mating surfaces are parallel in the region of Hertzian contact ($h \neq f(r_c)$) and the sliding velocity is constant then the coefficient of friction μ can be defined as;

$$\mu = F/w = \left(2\pi\eta_0\Delta u/(wh)\right) \times \int_0^a r_c \exp\left(\left(3w\alpha/2\pi a^2\right) \times \left(1-(r_c/a)^2\right)^{1/2}\right) dr_c \quad (6)$$

Equation (6) can be simplified under steady-state load (w) by the following;

$$\mu = \overline{c}\,\overline{I}\,\Delta u/h \quad (7)$$

where $\overline{I} = \int_0^a r_c \exp((3w\alpha/2\pi a^2)(1-(r_c/a)^2)^{1/2})dr_c$ and $\overline{c} = 2\pi\eta_0/w$.

3 Model friction and separation under starved lubrication

Under starved conditions the shear stress in Eq. (1) increases with increasing the sliding velocity, which leads to increase both of the traction force and the coefficient of friction. From Eq. (7) the coefficient of friction under starved conditions can be given as;

$$\mu_s = \overline{c}\,\overline{I}\,\Delta u/h_{cs} \quad (8)$$

where μ_s is the coefficient of friction under starved conditions and h_{cs} is the central film thickness of starved contact [m].

Chevalier *et al.* [8] introduced an approximated relation representing the ratio between the central film thickness under starved conditions and the central film thickness under fully flooded conditions by the following equation;

$$R = h_{cs}/h_{cff} = r/\sqrt[\gamma]{1+r^\gamma} \quad (9)$$

where the parameter $r = H_{oil}/\overline{\rho}H_{cff}$, $\overline{\rho}$ is the compressibility, if $\overline{\rho}$ is not considered then $r = H_{oil}/H_{cff}$. The parameter γ varies from 2 to 5. From Eq. (9) we can notice that the ratio $R \in [0, 1]$ as r changes from 0 to ∞. By substituting Eq. (9) in Eq. (8) we obtain the following relation;

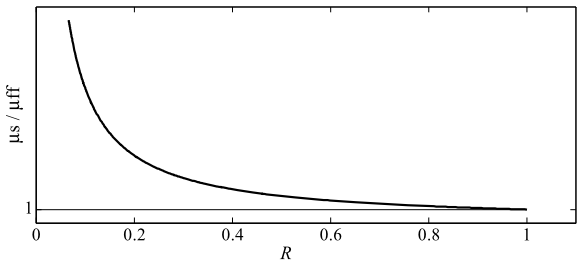

Fig. 1 The ratio μ_s/μ_{ff} versus the ratio $R = h_{cs}/h_{cff}$

$$\mu_s = \overline{c}\,\overline{I}\,\Delta u/Rh_{cff} \quad (10)$$

or

$$\mu_s = \mu_{ff}/R = \mu_{ff}\sqrt[\gamma]{1+r^\gamma}/r \quad (11)$$

where μ_{ff} and h_{cff} are respectively the coefficient of friction and the central film thickness under given operating conditions in the fully flooded lubrication.

Under steady state conditions, the coefficient of friction μ_{ff} has a constant value and the increase of starvation degree results in a nonlinear increase in the coefficient of friction μ_s under the same operating conditions according to Eq. (11).

Figure 1 shows the simulation of Eq. (11) and two asymptotes are observed. The first asymptote shows that the ratio μ_s/μ_{ff} tends to 1 as R tends to 1.

$$\lim_{R\to 1}(\mu_s/\mu_{ff}) = 1 \quad (12)$$

or

$$\lim_{R\to 1}(\mu_s) = \mu_{ff} \quad (13)$$

The other asymptote shows that the ratio μ_s/μ_{ff} tends to ∞ as R tends to 0. This situation represents the friction of dry contacts or boundary regime where the starved film thickness becomes 0.

$$\lim_{R\to 0}(\mu_s/\mu_{ff}) = \infty \quad (14)$$

Under severe starved lubrication, the film thickness may diminish to a few nanometers leading to the rise of air-oil meniscus in the inlet of contact. As the inlet meniscus approaches toward the circle of Hertzian contact, the gap between surfaces will be insufficiently filled by the fluid which inhibits the pressure build-up. If the contact is highly loaded and the pressure of fluid in the contact is low, then a part of the load will

be carried by the asperities and the regime of lubrication transforms from the EHD to the mixed lubrication (ML). However, the separation in the contact depends on the minimum film thickness and the roughness (RMS) of mating surfaces. To avoid the contact between asperities under starved lubrication, the film thickness parameter (λ) which was introduced by Tallian [16], should be larger than 1;

$$\lambda_{st} = h_{ms}/\sigma \geq 1 \tag{15}$$

where λ_{st} is the separation under starved conditions, h_{ms} is the minimum starved film thickness [m] and $\sigma = \sqrt{RMS_1^2 + RMS_2^2}$ where RMS_1, RMS_2 are the root mean square roughness of mating surfaces.

The ratio between central and minimum film thickness h_c/h_m tends to one under starved lubrication for all operating conditions. On the other hand, the ratio h_c/h_m tends to increase with load under fully flooded conditions, see Ref. [8] and references therein. We assume that $R' = h_{ms}/h_{mff}$ represents the ratio between the minimum film thickness of starved and fully flooded contact, where h_{mff} is the minimum film thickness of fully flooded contact. It is evident that the ratio $R' = (h_{ms}/h_{mff}) \in [0, 1]$ since the starved minimum film thickness cannot exceed the fully flooded minimum film thickness. By substituting $R' = h_{ms}/h_{mff}$ in Eq. (15) we obtain:

$$\lambda_{st} = R' h_{mff}/\sigma \geq 1 \tag{16}$$

$$\lambda_{st} = R' \lambda_{ff} \geq 1 \tag{17}$$

where λ_{ff} is the separation under fully flooded conditions. The last equation determines the conditions for keeping the contact under safe state against metal-to-metal contact through the transition from fully flooded to starved conditions. Equation (17) is simulated in Fig. 2 for different values of λ_{st}, where every curve in the figure represents a constant value of separation under starved lubrication conditions. Figure 2 shows that a constant starved separation ($\lambda_{st} = const$) results from a nonlinear relation between the degree of starvation and the fully flooded separation. For example, a fully flooded contact with a non-dimensional separation $\lambda_{ff} = 10$ can be starved to the degree $R' = 0.2$ which results in a starved separation $\lambda_{st} = 2$. On the other hand, the same starved separation $\lambda_{st} = 2$ can be obtained from a fully flooded separation $\lambda_{ff} = 4$ with the degree of starvation $R' = 0.5$.

However, in practical applications, safe operating conditions under starved lubrication require a minimum separation larger than the amplitude of surface

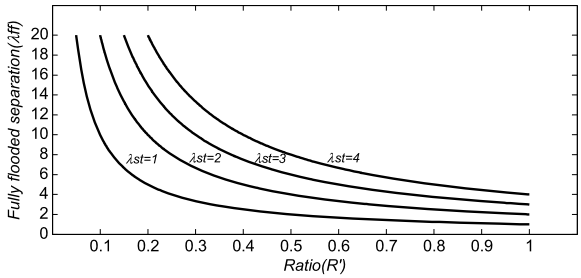

Fig. 2 Relation between the separation under starved and fully flooded conditions ($\lambda_{st}, \lambda_{ff}$) against $R' = h_{ms}/h_{mff}$

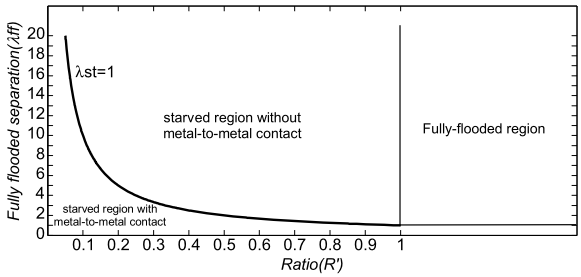

Fig. 3 Distribution of starved regions with and without metal-to-metal contact

asperities to avoid metal-to-metal contact; this case is defined in Fig. 3 where the region above the curve $\lambda_{st} = 1$ represents the safe separation whatever the degree of starvation was, and it can be stated that the friction in the region above the curve $\lambda_{st} = 1$ is basically due to the shear stress of the lubricant in sliding motion (see Eqs. (1), (6) and (7)) while the friction in the region under the curve $\lambda_{st} = 1$ is induced by the combined effect of the shear stress and metal-to-metal contacts.

4 Experimental

A tribometer modified by adding a torque sensor on the ball shaft was used for measuring the friction force between the ball and disk in the presence of base oil (2400 N) with a dynamic viscosity $\eta = 0.38$ [Pa s] at 40 °C. The torque sensor is integrated with a computer by using of Digital/Analog card (NI USB/6009) and the software LabVIEW receives the measurements as a digital signal to be processed and saved in the memory of the computer. The angular velocity of rotating parts is controlled by servo-motors where the velocity of ball can be independently changed in the

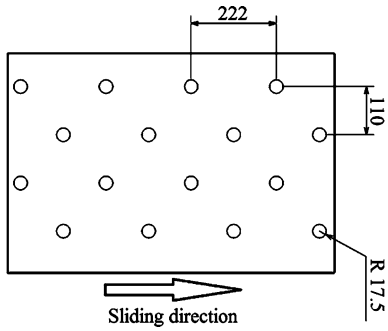

Fig. 4 Distribution of micro-dents on the surface of ball

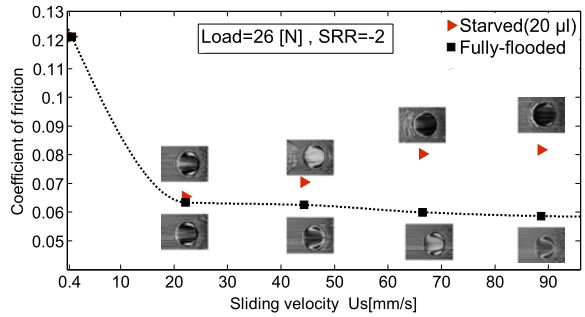

Fig. 5 Comparison of Stribeck curves for lubricated point contacts under starved and fully-flooded conditions

range −100 to +100 rpm, for disk the range is −150 to +150 rpm. This efficient mechanism provides the possibility of choosing the required slide-to-roll ratio under steady state and transient conditions. The diameter of ball is 25.4 [mm] and it is made of steel AISI 52100 with a measured roughness (RMS) about 15 nm, while the disk is made of a transparent glass and the lower surface of the disk is coated with a thin layer of Chromium. The elastic modulus of the steel ball and the glass disk is respectively 210 GPa and 80 GPa. On the other hand, the apparatus is equipped with a digital camera (Hitachi HV-F22) and the contact between the ball and disk is illuminated by a high-power source of light to improve the resolution of the images. This arrangement has the advantage of capturing interferometric images of the starved contact simultaneously with friction measurements by the torque sensor. The amounts of lubricant for starved conditions were calibrated by a digital micropipette.

For testing the effect of micro-dents on the coefficient of friction under starved conditions, the surface of the ball was manually indented by a Rockwell indenter. 4 rows were made along the whole ball circumference. Dents were made by applying a load of 8 N with the illustrated distribution in Fig. 4, where dimensions are in µm. The dent has an average diameter about 35 µm and a depth about 0.6 µm.

5 Results

The first part of results consists of experiments on friction under starved lubrication through non-steady state operating conditions (sliding velocity $u_s \neq const$) by establishing the Stribeck curve versus sliding velocity then experiments were conducted under steady state conditions by measuring the friction versus time, the effect of starvation on the position of inlet meniscus was investigated by optical interferometry. The second part provides an experimental comparison on the friction of textured and smooth non-conformal surfaces under starved and fully flooded conditions.

5.1 Stribeck curve

The coefficient of friction was measured versus the sliding velocity under pure sliding conditions ($SRR = 2 * (u_{disk} - u_{ball})/(u_{disk} + u_{ball}) = -2$, the disk is stationary $u_{disk} = 0$), the contact between the ball and disk was starved with oil amount 20 µl and it was loaded by 26 N. The measurements were repeated for the fully flooded contact with the same operating conditions and the position of the air-oil meniscus was simultaneously observed by digital camera. Figure 5 shows the measured Stribeck curves under starved and fully flooded conditions and it is evident that the air-oil meniscus approaches to the center of Hertzian contact as the sliding velocity increases because high velocities reduce the time needed to replenish the lubricant on the track where the oil is pushed out through sides by the over-rolling of the ball. The frequency of over-rolling determines the amount of oil that can flow back into the track, hence, the efficiency of oil replenishment on the track is inversely proportional to the frequency of over-rolling. In other words, high frequency of over-rolling at high sliding velocities leads to increase the degree of starvation and the reduction of film thickness due to the reduction of replenishment time. However, the comparison of the friction coefficient between starved and fully flooded conditions shows that the value of the friction coefficient increases strongly with increasing the sliding velocity

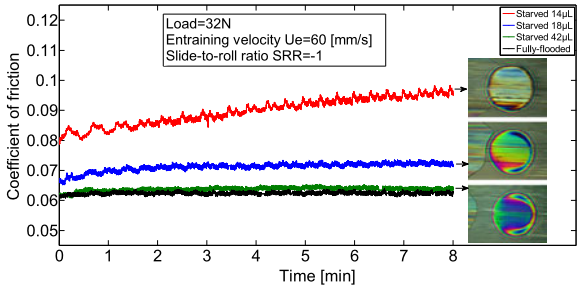

Fig. 6 Effect of oil amount on the coefficient of friction and the position of air-oil meniscus

under starved conditions, on the contrary, under fully flooded conditions, it is clear from Fig. 5 that high velocities enhance the film thickness and the separation according to the EHL theory, which results in low friction. The existence of the meniscus in the vicinity of the Hertzian contact reduces the pressure build-up of fluid and inhibits the formation of film lubrication in the contact which increases the contact between the asperities and the friction. Otherwise, it is observed that there is not such a large difference in the friction coefficient for starved and fully flooded conditions as the air-oil meniscus is far enough from the center of Hertzian contact at low sliding velocities.

5.2 Steady state

The effect of air-oil meniscus position on the coefficient of friction was observed under steady state operating conditions of the sliding and load ($SRR = -1$, entraining velocity $u_e = |u_s| = 60$ [mm/s], load = 32 N) and the degree of starvation was modified by changing the oil amount on the track, see Fig. 6 and please note that the images were captured in the 5th minute. Interferometric images show that the coefficient of friction increases significantly under starved conditions when the air-oil meniscus starts to touch the Hertzian contact. Otherwise, the coefficient of friction of starved and fully flooded contact is nearly the same for a sufficient amount of oil (42 µl) on the track. The rapid increase of the friction coefficient is attributed to the insufficient replenishment of fluid on the track for the little amount of lubricant which results in reducing the distance between the air-oil meniscus and the center of Hertzian contact. However, it is apparent that a little reduction of oil amount from 18 µl to 14 µl caused a large increase of friction, so it can be stated that, as the inlet meniscus is in touch with the Hertzian circle the gradient of friction becomes very sensitive and related to the oil amount on the track, while the effect of oil amount on the value of friction is quite fair since the inlet meniscus is out of the Hertzian circle. This result is in agreement with the theoretical model shown in Fig. 1, and it is clear from Fig. 1 that the gradient of the ratio μ_s/μ_{ff} is very little when the degree of starvation is low ($R \approx 1$) then the gradient starts to increase rapidly with increasing the degree of starvation ($R \ll 1$) and it is expected that the accelerated increase starts in the moment at which the air-oil meniscus starts to touch the Hertzian contact. If we assume that the degree of starvation at which the inlet meniscus starts to touch the Hertzian circle is the critical degree of starvation (R_{cr}) then we can explain mathematically the behavior of friction gradient versus the degree of starvation by the following;

$$\left|\Delta(\mu_s/\mu_{ff})/\Delta R\right| \approx 0 \quad \text{if } 1 \geq R \geq R_{cr} \tag{18}$$

$$\left|\Delta(\mu_s/\mu_{ff})/\Delta R\right| > 0 \quad \text{if } R < R_{cr} \tag{19}$$

Equation (18) represents the range of starvation where the inlet meniscus is far away from the contact, in this range of starvation, friction shows a low sensitivity against the small change of oil amount on the track, while Eq. (19) represents the range of starvation where the inlet meniscus is in interference with the Hertzian contact and the high sensitivity of friction against the small change of oil amount on the track.

In practical applications, it is difficult to determine the precise position of the inlet meniscus and the critical degree of starvation R_{cr} at which the inlet meniscus starts to touch the Hertzian circle, but on the basis of Eqs. (18) and (19) it is possible to determine approximately the fuzzy place of R_{cr} by using the coefficient of friction as indicator to the moment at which the air-oil meniscus makes the first contact with the Hertzian circle, see Fig. 7. However, the accuracy of determining the approximated place of R_{cr} depends on the ranges defined by Eqs. (18) and (19) in Fig. 7 and more expanded experimental tests are needed to precise correctly these ranges.

The experimental relation between the ratio μ_s/μ_{ff} and the amount of oil is represented in Fig. 8 where the values of μ_s and μ_{ff} were calculated from the mean value during 8 minutes of measuring. The experimental ratio μ_s/μ_{ff} tends to one as the degree of starvation reduces and we can clearly notice the accelerated increase of friction gradient at little amounts of oil (the jump of friction between values 18 µl and 14 µl).

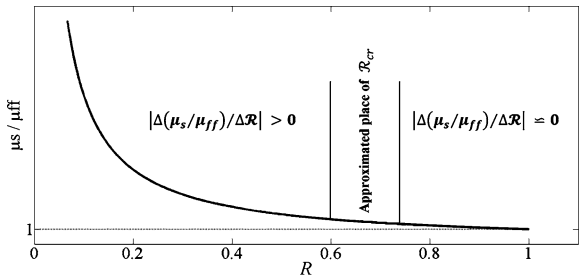

Fig. 7 Approximated approach to determine the critical degree of starvation R_{cr}

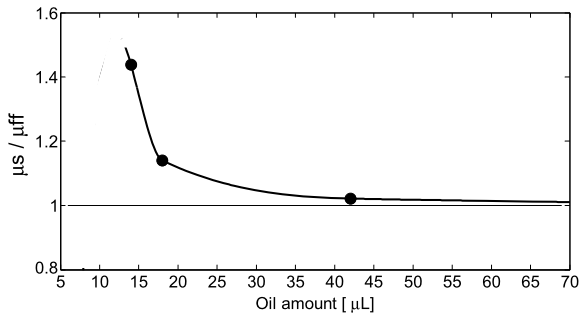

Fig. 8 Experimental relation between the ratio μ_s/μ_{ff} and the oil amount on the track

However, this result is in accord with Fig. 1 and Eqs. (12) and (13). The good agreement between the theoretical model in Fig. 7 and the experimental measurement in Fig. 8 is not absolute because the theoretical model was derived from the Newtonian model in the shear stress regardless rheological properties of the lubricant, for this reason, an optimized model which takes in account the non-Newtonian behavior of oil can be more realistic. In addition to that, the theoretical model is correct under steady state operating conditions but it cannot be adopted for non-steady states or transient cases.

5.3 Friction of textured surfaces

The study above indicated that the coefficient of friction becomes very sensitive to the little change of oil amount when the degree of starvation is large; this region is presented in Fig. 7 by the formula $|\Delta(\mu_s/\mu_{ff})/\Delta R| > 0$. According to this result, it is expected that the surface texturing to be efficient in this region because the little amount of oil emitted from micro-dents can play a significant role in reducing the friction. In contrast, it is not recommended to apply the surface texturing under fully

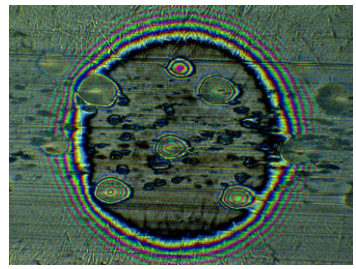

Fig. 9 Micro-dents on the ball surface

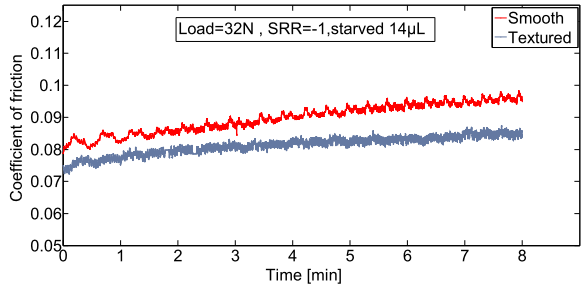

Fig. 10 Coefficient of friction for smooth and textured surfaces under starved conditions

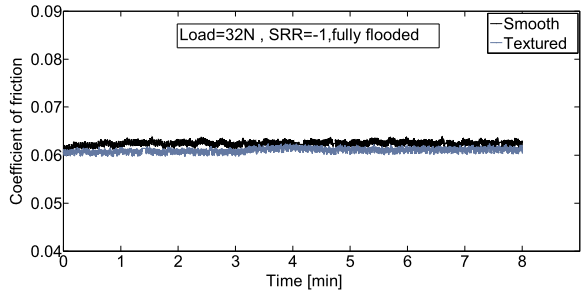

Fig. 11 Coefficient of friction for smooth and textured surfaces under fully flooded conditions

flooded or fairly starved conditions where the coefficient of friction is insensitive to small changes of oil amount, this case is presented in Fig. 7 by the formula $|\Delta(\mu_s/\mu_{ff})/\Delta R| \approx 0$.

However, in order to investigate the effect of micro-dents in reducing the friction, the surface of the ball was artificially modified by 4 rows of shallow micro-dents, see Fig. 9. The average diameter of the dent is about 35 μm with a depth about 0.6 μm.

Figures 10 and 11 show a comparison of the friction coefficient for smooth and textured surface under starved and fully flooded lubrication. Results show that the benefits of micro-dents under severe starved

lubrication are proportionally considered and the reduction of friction is about 9 %. On the other hand, the benefits of micro-dents under fully flooded conditions are negligible and the value of average friction of smooth and textured surfaces is nearly the same; this is justified by the fact that the little amount of emitted fluid from micro-dents doesn't make a significant difference in enhancing the film thickness under fully flooded lubrication where the film is originally large enough. In addition to that, it was mentioned in the context of this study that coefficient of friction is insensitive against the micro-change in oil amount under fairly starved and fully flooded conditions.

From Figs. 10 and 11 we can also notice that the friction increases with the time under steady state for both textured and smooth surfaces under starved lubrication while the friction is stable with the time under fully flooded condition and this can be attributed to the thermal effect where the available amount of oil under fully flooded condition is larger in comparison with the starved condition which results in a larger heat capacity for fully flooded contact, for this reason the oil temperature for starved conditions is higher than the oil temperature for fully flooded conditions under the same operating conditions.

6 Conclusions

The friction coefficient of non-conformal EHL point contacts was measured under starved and fully flooded conditions and the benefits of surface texturing were also investigated. Results show that the friction coefficient of non-conformal point contacts increases dramatically and non-linearly under starved conditions when the sliding velocity increases; this action is accompanied by reducing the time to replenish the lubricant on the track which results in minimizing the distance between the air-oil meniscus and the center of Hertzian contact. Under steady state conditions, the coefficient of friction depends strongly on the oil amount on the track, particularly at high degrees of starvation. On the other hand, the value of the friction coefficient was almost the same for fully flooded and starved contacts when the air-oil meniscus was far away from the Hertzian contact. Results showed a good agreement between the theoretical model of friction under starved lubrication and experimental measurements, this theoretical model can be used to predict approximately the position of inlet meniscus. Finally, the modification of non-conformal mating surfaces by shallow micro-dents provided a considerable reduction of friction (about 9 %) under severe starved lubrication while the benefits of micro-dents were negligible for fully flooded lubrication.

Acknowledgement This research was supported by Czech Science Foundation (project No. GA101/11/1115) and European Regional Development Fund (project No. CZ.1.07/2.3.00/20.0126) financed.

References

1. Hamrock BJ, Dowson D (1977) Isothermal elastohydrodynamic lubrication of point contacts. Part III—fully flooded results. J Lubr Technol 99:264–276
2. Dowson D, Higginson GR (1959) A numerical solution to the elastohydrodynamic problem. J Mech Eng Sci 1:6–15
3. Wedeven LD, Evans D, Cameron AC (1971) Optical analysis of ball bearing starvation. ASME J Lubr Technol 93:349–363
4. Elrod HG (1981) A cavitation algorithm. ASME J Lubr Technol 103:350–354
5. Elrod HG, Adams ML (1974) A computer program for cavitation and starvation problems. In: Proceedings of the 1st Leeds-Lyon symposium on tribology, pp 37–41
6. Chiu YP (1974) An analysis and prediction of lubricant film starvation in rolling contact systems. ASLE Trans 17:22–35
7. Pemberton J, Cameron AC (1976) A mechanism of fluid replenishment in elastohydrodynamic contacts. Wear 37:185–190
8. Chevalier F, Lubrecht AA, Cann PME, Colin F, Dalmaz G (1998) Film thickness in starved EHL point contacts. ASME J Tribol 120:126–133
9. Lubrecht T, Mayuzer D, Cann P (2001) Starved elastohydrodynamic lubrication theory: application to emulsions and greases. C R Acad Sci, Sér IV Phys Astrophys 2(5):717–728
10. Cann PME, Damiens B, Lubrecht AA (2004) The transition between fully flooded and starved regimes in EHL. Tribol Int 37:859–864
11. Damiens B, Venner CH, Cann PME, Lubrecht AA (2004) Starved lubrication of elliptical EHD contacts. ASME J Tribol 126:105–111. doi:10.1115/1.1631020
12. Wedeven LD (1975) Traction and film thickness measurements under starved elastohydrodynamic conditions. Trans ASME J Lubr Technol 97:321–329
13. Querlioz E, Ville F, Lenon H, Lubrecht T (2007) Experimental investigations on the contact fatigue life under starved conditions. Tribol Int 40:1619–1626
14. Yang P, Wang J, Kaneta M (2006) Thermal and non-Newtonian numerical analyses for starved EHL line contacts. ASME J Tribol 128:282–290
15. Barus C (1893) Isothermals, isopiestics and isometrics relative to viscosity. Am J Sci 45:87–96

16. Tallian TE (1967) On competing failure modes in rolling contact. ASLE Trans 10:418–439
17. Nakatsji T, Mori A (2001) The tribological effect of mechanically produced micro-dents by a micro diamond pyramid on medium carbon steel surfaces in rolling-sliding contact. Meccanica 36:663–674
18. Coulon S, Jubault I, Lubrech AA, Ville F, Vergne P (2004) Pressure profiles measured within lubricated contacts in presence of dented surfaces. Comparison with numerical models. Tribol Int 37:111–117
19. Nelias D, Ville F (2000) Detrimental effects of debris dents on rolling contact fatigue. Trans ASME J Tribol 122:55–64
20. Mourier L, Mazuyer D, Lubrecht AA, Donnet C (2006) Transient increase of film thickness in micro-textured EHL contacts. Tribol Int 39:1745–1756
21. Ai XL, Cheng HS (1994) The influence of moving dent on point EHL contacts. Tribol Trans 37:323–335
22. Krupka I, Hartl M (2007) The effect of surface texturing on thin EHD lubrication films. Tribol Int 40:1100–1110
23. Vrbka M, Křupka I, Šamánek O, Svoboda P, Vaverka M, Hartl M (2011) Effect of surface texturing on lubrication film formation and rolling contact fatigue within mixed lubrication. Meccanica 46:491–498
24. Galada L, Dzierwa A, Pawlus P, Reizer R (2011) Improvement of tribological properties of co-elements by oil pockets creation on sliding surfaces. Meccanica 46:523–534
25. Dumont M, Lugt PM, Tripp JH (2002) Surface feature effects in starved circular EHL contacts. Trans ASME J Tribol 124:358–366